Supplementary Materials: Effective Electrons Transfer Pathway of the Ternary TiO_2/RGO/Ag Nanocomposite with Enhanced Photocatalytic Activity under Visible Light

Hongwei Tian, Chenxing Wan, Xin Xue, Xiaoying Hu, Xiaoyi Wang

Table S1 summarizes the specific surface area, pore diameter of various samples. The average pore size of MTGA-8 was 8.08 nm in the range of allowable error compared with MT and MTGA, which implies that the decoration of Ag nanoparticles basically does not destroy the original structure. Among all of the prepared photocatalysts, the BET surface area of the MTGA-8 catalyst was found to decrease to 119 m^2/g; however, the photocatalytic activity of MTGA-8 is the best compared with MTG and MT, perhaps because the deposition of Ag nanoparticles blocks part of the channels, resulting in the decrease in specific surface area, but enhancing light absorption and electron transfer due to the LSPR effect of Ag nanoparticles [1].

Table S1. Textural properties of MT, MTG and MTGA-8 nanocomposites.

Catalysts	Specific Surface Area (m^2/g)	Pore Diameter (nm)
MT	146	8.39
MTG	145	8.24
MTGA	119	8.08

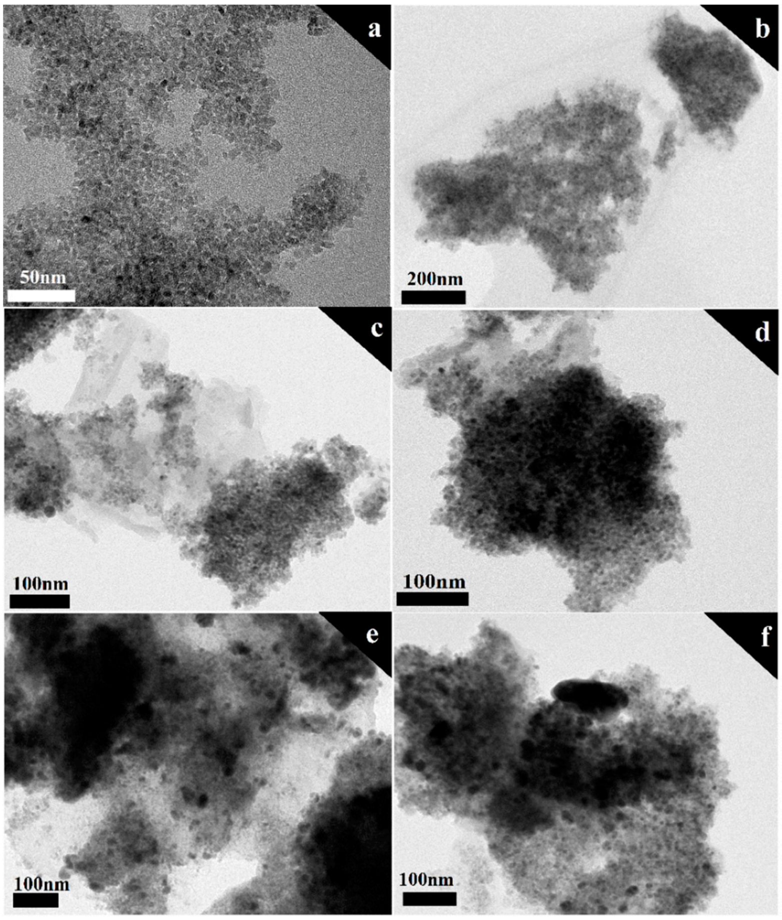

Figure S1. TEM images of MT (**a**), MTG (**b**), MTGA-3 (**c**), MTGA-5 (**d**), MTGA-8 (**e**) and MTGA-10 (**f**) nanocomposites.

The similar results as for the SEM images in Figure 5 also appear in the TEM images shown in Figure S1. Figure S1a shows the TEM image of MT, from which we can see that there are worm-like channels between MT nanoparticles, which is additional powerful evidence for the mesoporous structure of TiO_2. Additionally, by electrostatic self-assembly, you can clearly see the MT particles modified on the thin RGO nanosheets in Figure S1b. Then, we use the photo-assisted depositing of Ag nanoparticles, and Figure S1c–f shows the TEM images of the ternary MTGA with different amounts of Ag loading. All of the figures show similar distributions, which is that the aggregated MT adheres to the cotton-like RGO nanosheets, and Ag nanoparticles are located on the MT. When increasing Ag loading, the distribution of Ag nanoparticles is widened. From Figure S1e, we can see that Ag nanoparticles evenly disperse throughout the region, and the particle size is about 10–20 nm. In addition, with continuing to increase the amount of Ag, Ag nanoparticles are agglomerated, as shown in Figure S1f.

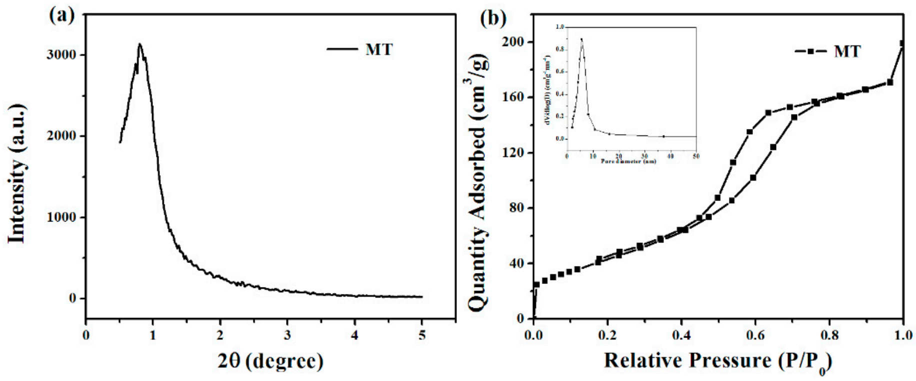

Figure S2. XRD pattern in small-angle (**a**), nitrogen sorption isotherm (**b**) and the corresponding pore size distribution curve (inset) for MT.

The fact that TiO_2 with a mesoporous structure possesses a large surface area is proven by the small-angle XRD pattern and nitrogen sorption isotherm of MT. The small-angle XRD pattern for MT in Figure S2a can also prove the existence of mesopores [2]. Furthermore, based on the nitrogen sorption isotherm in Figure S2b, we can see that the isotherm of the MT nanocomposite belongs to type IV with the H2 hysteresis loop, and the specific surface area of the MT nanocomposite is investigated respectively to be 146 $m^2\,g^{-1}$. In addition, the pore size mainly ranges from 2–20 nm, as shown in the inset of Figure S2b.

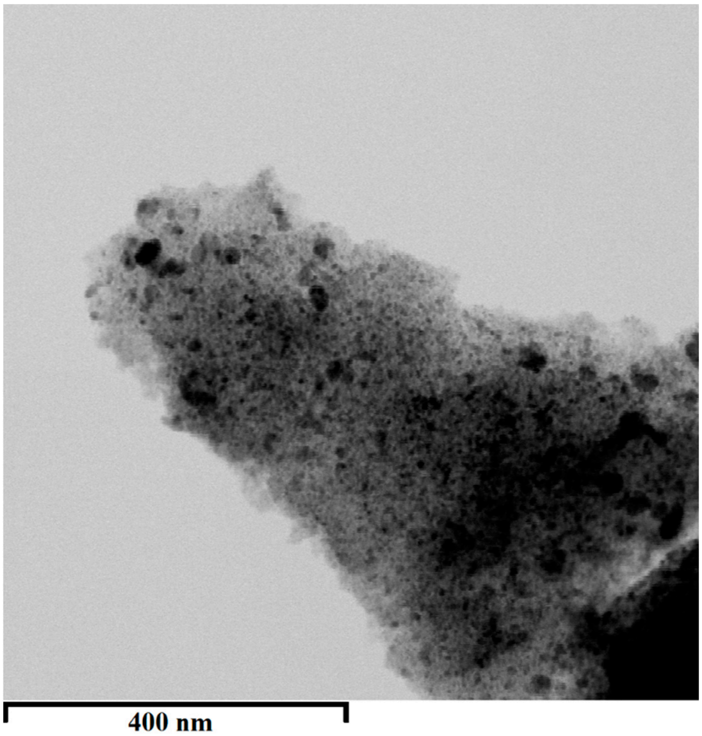

Figure S3. The selected pattern with the elemental mapping of the MTGA-8 nanocomposite.

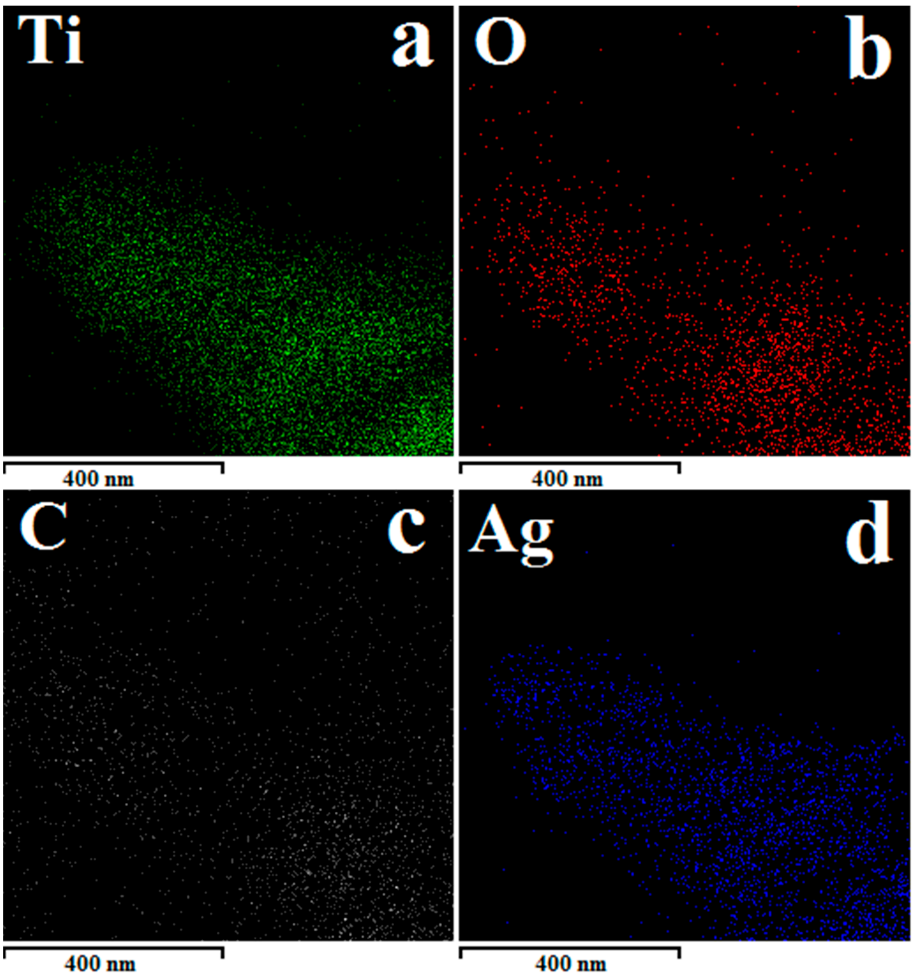

Figure S4. The corresponding elemental mapping images of Ti (a), O (b), C (c) and Ag (d).

Figure S4a–d displays the elemental mapping images based on the selected area (Figure S3) on behalf of the Ti, O, C and Ag elements; it is further side evidence that Ag nanoparticles are deposited successfully by the photo-assisted process.

Table S2. The apparent reaction rate constants k in the presence of visible light of MT, MTG and MTGA nanocomposites.

Catalysts	MT	MTG	MTGA-3	MTGA-5	MTGA-8	MTGA-10
K/min^{-1}	0.00151	0.00519	0.01141	0.01003	0.01742	0.01288

Table S2 presents the apparent reaction rate constants k under visible light of the samples. The k of MTGA-8 is 0.017 min^{-1}, the highest value of all samples, which is 3.4-times the degradation rate of MTG.

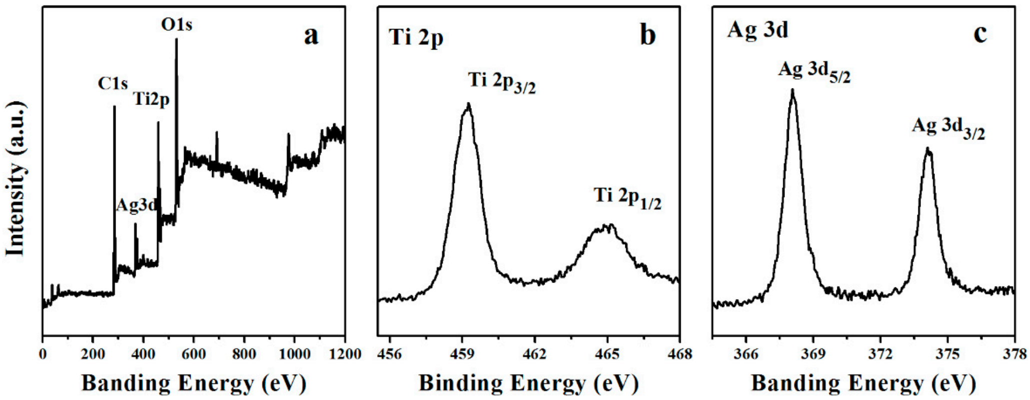

Figure S5. XPS spectra of survey (a), Ti 2p (b) and Ag 3d (c) for the MTGA nanocomposite after three cycle times.

XPS spectra for MTGA nanocomposite can also prove this fact. Figure S5a shows the existence of the elements Ti, Ag, O and C in the MTGA nanocomposite after three cycle times. What is more, the peak positions of Ti and Ag in Figure S5b,c are identical to Figure 4a,b, which indicates that degradation has no effect on Ti-O-C bonds [3]; and the state of silver remains metallic silver (Ag^0) [4].

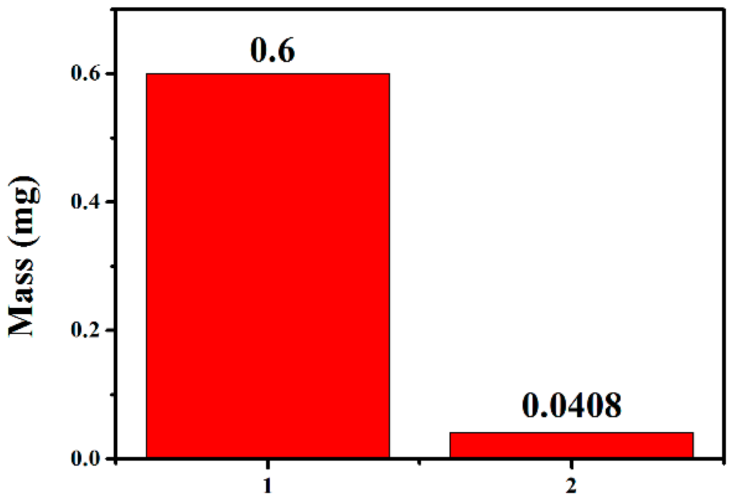

Figure S6. The mass of MB before and after degradation.

Figure S6 presents the mass of MB before and after degradation. In the experiment of the degradation of MB, we added MTGA nanocomposite to 60-mL, 10-mg/L MB solution (the original mass of MB is 0.6). When irradiating 120 min by visible light, the degradation rate (C/C0, C and C0 refer to the concentration of the solution at a given time and the concentration of the original solution, respectively) reaches 93.2%. According to these data, we calculate that the mass of MB reduced to 0.0408 mg after degradation.

References

1. Qu, Y.; Duan, X. Progress, challenge and perspective of heterogeneous photocatalysts. *Chem Soc Rev.* ***2013***, 42, 2568–2580. doi:10.1039/c2cs35355e.
2. Li, G.S.; Zhang, D.Q.; Yu, J.C. A new visible-light photocatalyst: CdS quantum dots embedded mesoporous TiO_2. *Environmental Science & Technology* **2009**, 43, 7079–7085. doi:10.1021/es9011993.
3. Wang, W.S.; Wang, D.H.; Qu, W.G.; Lu, L.Q.; Xu, A.W. Large ultrathin anatase TiO_2 nanosheets with exposed {001} facets on graphene for enhanced visible light photocatalytic activity. *J. Phys. Chem. C* **2012**, 116, 19893–19901. doi:10.1021/jp306498b.
4. Xiao, F. Layer-by-layer self-assembly construction of highly ordered metal-TiO_2 nanotube arrays heterostructures (m/tnts, m = au, ag, pt) with tunable catalytic activities. *J. Phys. Chem. C* **2012**, 116, 16487–16498. doi:10.1021/jp3034984.